A Low-Cost Earth Imaging System

Thomas H. Zurbuchen, Ryan A. Falor, Romain Clement, Daniel Paul, and Robby Swoish
Department of Atmospheric, Oceanic and Space Sciences and Department of Aerospace Engineering
University of Michigan
2455 Hayward St.
Ann Arbor, MI 48109
734-647-6835
thomasz@umich.edu, aerofalor@gmail.com, clemrom@gmail.com, pauldj@umich.edu, rswoish@umich.edu

Thomas Ryan
EDM Technical Services
1517 E Park Pl.
Ann Arbor MI 48104
tpryan@provide.net

Abstract—Observations of the Earth from space have primarily been dominated by applications that require very accurate pointing to specific locations of interest, with high reliability and small latency. However, today the general public has access to high-resolution imagery on a scale never before imagined. Acquiring large data sets of Earth imagery in a simple, low-cost way, represents a new market opportunity that has yet to be addressed. It is the purpose of this paper to discuss a telescope design that is part of a low-cost satellite with that purpose. The system uses a fast, two-mirror optical design with push-broom imaging. The design of the telescope involves innovative technologies to reduce costs without impacting the optical performance of the system. This paper will include a detailed theoretical performance analysis, as well as discussions of the test strategy and manufacturing approach that make this telescope very cost effective.[1] [2]

TABLE OF CONTENTS

1. INTRODUCTION

The use of Earth imaging from space is undergoing an important transition [see details in 1]. There is a new demand for high-resolution imagery on an unprecedented scale. Pioneering efforts on the internet are spawning a whole industry of GIS content services. These new services are fueling the demand for world-wide imagery. To meet this demand a new approach to satellite imagery is required, one that no longer fits the standard military point-and-shoot model. Instead of providing dozens of images of highly targeted scenes during a given orbit, our system will provide hundreds or thousands of images each orbit using a push-broom method. The system approach relies on an "image-as-we-go" technique to maximize usable imagery. Consequently, the system will allow for coverage of the entire inhabited Earth in approximately one year. This timescale arises from the necessity to stay current and keep up with construction projects and other evolutionary aspects of the Earth. Five-color images, such as those provided by Landsat [2], are sufficient, and they can be adjusted on the ground to be consistent with neighboring data sets. Furthermore, a resolution of 60 cm (pixel resolution) is desired to match the current resolution of imagery available from other commercial sources, such as DigitalGlobe [3].

The telescope payload drives all other system requirements for an imagery mission. The mass and volume required for the telescope set the size and complexity of the spacecraft bus. The optics and resolution requirements drive the orbit altitude, which in turn affects lifetime and data rates. Increasing the size of the optics dramatically increases cost and structural concerns, while reducing the optics lowers the resulting resolution. Optimization of these competing requirements was done through a series of system-level trades and multiple design iterations [4, 5]. The analysis indicated that the target performance requirements could be achieved with a 460-km altitude sun-synchronous orbit [1]. Table 1 shows the overall requirements for the GoBlue

[2] IEEEAC paper #1430, Version 1, November 14, 2006

Table 1. Overall system requirements for the GoBlue telescope.

Resolution (panchromatic)	1.2 m
Ground sampling distance (panchromatic)	0.6 m
Resolution (multispectral)	1.8 m
Ground sampling distance (multispectral)	0.9 m
Orbit type	Sun-Synchronous
Orbit altitude	460 km
Field of view (FOV) half-angle	1.148 degrees
Primary mirror aperture	0.60 m
F ratio (F/ #)	F/5.53
Focal length	3.32 m
Pixel size (panchromatic)	8.75 µm
Pixel size (multispectral)	13 µm
Spectral range	400-700 nm
CCD type	Time delay integration
Image quality	Diffraction limited
Acceptable MTF contrast amplitude	> 30%
Maximum quasi-static acceleration (on axis)	9 g's
Maximum quasi-static acceleration (lateral)	2 g's
Acceptable factor of safety (ultimate stress)	2.0
Acceptable factor of safety (yield stress)	1.5
Thermal range	-20^{o}C-60^{o}C

telescope as defined by this orbit selection. These requirements are explained in detail in the remainder of the report.

This telescope design has been developed in a three-semester sequence in a Professional Space Systems program at the University of Michigan. The design effort involved approximately fifty individuals at the University of Michigan and a number of outside consultants, with leading roles by the authors. This paper summarizes the findings of this study, which addressed all key aspects of the space system, developed under the name of "GoBlue Imager" (GBI), using the SMAD process by [6]. One critical requirement for this analysis was the cost of the space system. Our intention was to simplify telescope manufacturing and testing processes in order to keep costs to a minimum. This resulted in design trades that are unusual for high-resolution remote-sensing applications for reconnaissance and many scientific applications which require highly calibrated data sets.

2. GoBlue Telescope Overview

Several two- and three-mirror telescope designs were considered for this application. Three-mirror designs, specifically the Three-Mirror Anastigmatic (TMA) design, allowed for a more compact imaging system with a larger flat field and not only coma and spherical aberration correction but also stigmatic and chromatic aberration correction [7]. Two-mirror systems have simpler designs and, with the right structural design, require less mass both in terms of mirror mass and structural support mass. These designs are symmetric and easier to align than a comparable TMA. However, they have longer dimensions and require lenses to correct for aberrations that a TMA already corrects for. Because of the costs associated with maintaining mirror alignment in a multi-axis, three-mirror system subject to thermal cycling and vibration, we have determined that a two-mirror design with lenses would offer the best performance for the development price.

The Ritchey-Chrétien design was chosen over three other commonly employed two-mirror telescope designs (Newtonian, Cassegrain, and Schmidt-Cassegrain) based on its superior aberration correction capabilities [8]. The Ritchey-Chrétien telescope design employs hyperbolic mirrors that allow for the correction of both coma and spherical aberrations, whereas the other three designs considered have parabolic and/or spherical mirror surfaces that only allow for the correction of either coma or spherical aberration.

2.1 Telescope Overview

This section focuses on three aspects, which will be explained later. We first focus on the overall functionality of the telescope, then the overall structural design, and finally the focal plane design of the telescope for which staggered CCDs were used.

Figure 1 shows the system layout of the GoBlue telescope for a ZEMAX raytrace over the full field of view (0.000^o, 0.250^o, 0.500^o, 0.750^o, 1.000^o, and 1.148^o). The concave, hyperbolic (conic constant = -1.197) primary mirror is 60 cm in diameter, and it reflects light back to the secondary, which is a convex hyperbolic (conic constant = -7.37) mirror with a diameter of 22 cm. The shapes of both mirrors were chosen based on manufacturability and cost. The primary and secondary mirrors provide sufficient on-axis resolution; however, a refractive group is required to flatten the field and maintain the required resolution over the full field of view, as required in Table 1.

Figure 2 shows the mechanical structure of the optical elements and baffles that are used for background light suppression and for structural reasons. There are two baffles. The baffle around the secondary eliminates stray radiation from the structure of the telescope, which is shaped to minimize stray-light reflection. A second baffle surrounds the refractive group. This baffle also has structural integrity to keep all refractive elements in place. The structure was designed to maintain the positioning of the optics through the launch loads and thermal range as outlined in Table 1, in order to maintain the designed image

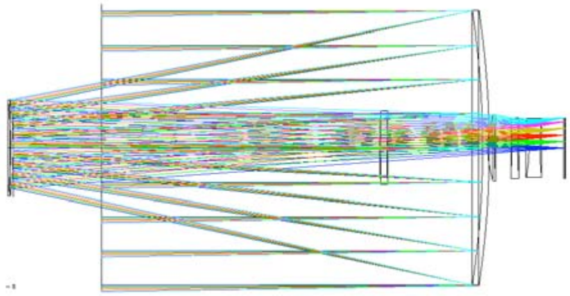

Figure 1. GoBlue telescope layout. The telescope consists of a 60-cm primary mirror and a secondary with a refractive group, with a field of view as required in Table 1. Color traces correspond to off-axis field-of-view angles (blue=0.000°, green=0.250°, red=0.500°, yellow=0.750°, pink=1.000°, light blue=1.148°).

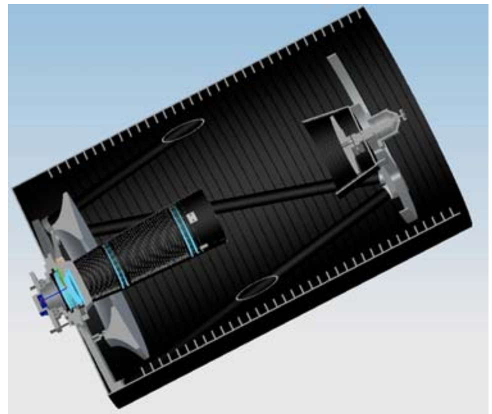

Figure 2. GoBlue mechanical layout. A baffle near the secondary mirror eliminates off-axis scattered photons.

Table 2: Geometrical description of geometry and make of the GoBlue telescope optical components. For definitions of the materials, see [11].

Optical Surface	Material	Diameter (mm)	Central hole (mm)	Radius of Curvature (mm)	Conic Constant	Central Thickness (mm)
Primary	Zerodur®	600	260	2400	-1.197	85
Secondary	Zerodur®	220	15	1178	-7.37	23.5
Lens 1- S1	SF14	172	None	2585	0	17
S2				2515		
Lens 2- S1	N-BAK2	151	None	686	0	14
S2				2205		
Lens 3- S1	LF5	127	None	260	0	14
S2				163		
Lens 4- S1	N-SSK5	125	None	159	0	20
S2				825		

quality and resolution (Table 1). The mechanical structure has a three-fold symmetry, holding the telescope in place by three structural elements that are almost identical.

2.2. Telescope Design

The mission design orbit altitude and desired resolution drive the system size and complexity. With an orbital altitude of 460 km, a CCD with pixels 8.75 µm x 8.75 µm (panchromatic), and a clear aperture diameter of 60 cm, the telescope can resolve 2.4-m resolution (1.2-m ground sampling resolution). Our design however incorporates two TDI CCD arrays staggered at half of a pixel length, which effectively halves the resolution (1.2-m or 0.6-m ground sampling resolution) [9].

This aperture requirement drives the diameter of the primary mirror, which usually accounts for a large fraction of the telescope mass. Our primary mirror has a concave, F/2 hyperbolic surface with a double-arch back to reduce mass. It is made of Zerodur®, due to that material's low thermal expansion properties. The convex hyperbolic secondary mirror is also made of Zerodur® with a single-arch back design. Table 2 gives physical properties and dimensions of the mirrors, as well as those for the four correction lenses. Each lens is made of a different Schott glass that is commercially available and can withstand the space environment.

The focal plane of the telescope includes two panchromatic and three multispectral band CCD detectors. Table 3 describes the overall dimension of the CCDs, which are run in a time-delay integration mode [10]. Three CCDs for separate spectral bands are placed in the focal plane. The highest-resolution data come from the panchromatic CCDs, and are achieved by using the two identical CCDs in a staggered configuration.

Table 3: Geometrical properties of panchromatic and multispectral CCDs used in the telescope.

	Multispectral	Panchromatic
Number of pixels	4100	6144
Pixel size [µm]	13	8.75
Length of CCD's active zone [cm]	5.32	5.38
CCD chip width [cm]	1.52	3.05
CCD chip length [cm]	6.35	11.8

Figure 3 explains the principle of the staggered CCD concept that is being used here to double the sampling frequency [see, 9]. In a linear CCD, as shown in black, the sampling frequency is $1/\Delta_{pix}$, where Δ_{pix} denotes the distance between the centers of two neighboring pixels in a given row. In a staggered configuration, a second identical CCD is placed immediately next to the first CCD, with an offset of one half of a pixel, as sketched in red in Figure 3. Due to the push-broom function of the telescope, the pixels of the two neighboring CCDs can be interleaved in software, leading to an effective doubling of the resolution. The conclusions for our design are obvious: In the direction of the push-broom, a staggered CCD whose pixels are 13-µm wide is equivalent to a linear CCD with 13/2 = 6.5-µm large pixels while preserving the area of 13^2 = 169 mm^2 per pixel, thus increasing the sensitivity.

Two adjustment mechanisms have been designed to allow for positioning corrections while in orbit. The first mechanism allows motion of the secondary mirror along the system's symmetry axis and for tilts relative to it. The second mechanism moves the focal plane in a similar manner. These mechanisms alleviate some of the strict positioning requirements on both the secondary mirror and focal plane position. Detailed thermal analyses using ZEMAX and mechanical design software reveal that adjustment of both the secondary mirror and focal plane is necessary to maintain a 30% MTF contrast amplitude over the full 1.148^{o} field of view.

Detailed optical and mechanical properties are discussed in the next sections, followed by a discussion of the test strategy and the manufacturing approach used for this system.

3. Optical Performance

The Ritchey-Chrétien (RC) design, utilizing hyperbolic primary and secondary mirrors, alone does not satisfy the requirements for this telescope system. Although an RC design corrects for coma and spherical aberration, stigmatic and chromatic aberrations must also be corrected. Given the number and size of the TDI CCD chips (2 staggered panchromatic and 3 multispectral detectors) the size of the focal plane must be 13.5 cm in diameter, adding important constraints to the design. In order to correct for the stigmatic and chromatic aberrations and to increase the size of the flat field on the focal plane, lenses had to be added to the system. Optimization of the optics for this modified Ritchey-Chrétien telescope was done using the ZEMAX optical design program. The resulting design incorporates four lenses that correct for the stigmatic and chromatic aberrations and increases the flat field size over the focal plane. In order to maintain a low-cost system, the lenses were designed with commercially available materials from the Schott catalog [11].

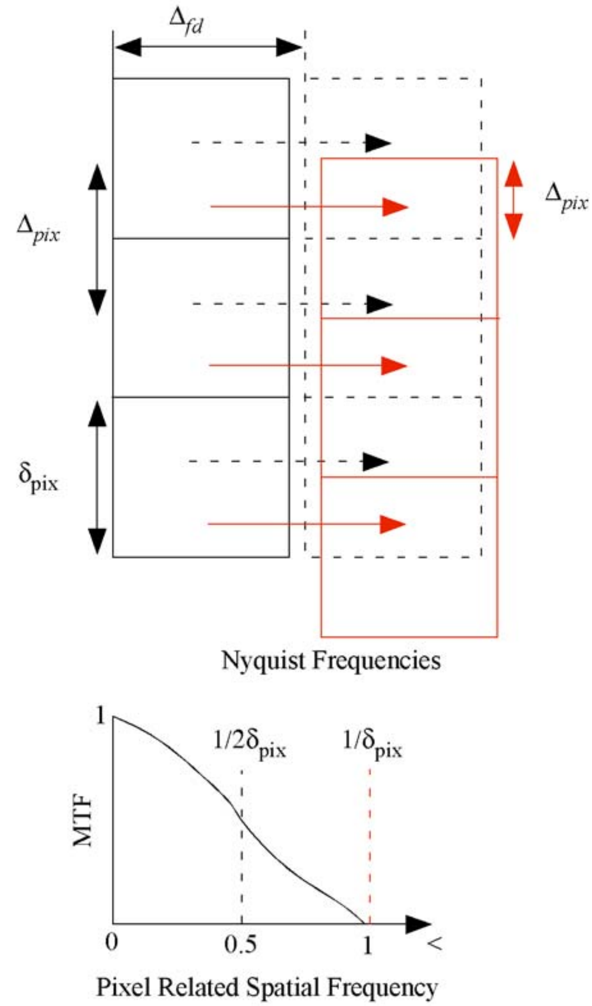

Figure 3. Sampling and Nyquist frequency for linear and staggered CCD-line according to [9]. For discussion, refer to text.

The two main measures to assess the resolution of the telescope are the Modulation Transfer Function (MTF) and the spot diagrams. The MTF is a quantitative measure of image quality describing the ability of an optical system to transfer object contrast to the image. An MTF relates the working spatial frequency of the optics, in units of line pair cycles per millimeter, to the percentage of the contrast measured from the original image.

The telescope must be designed so that the working spatial frequency of the MTF remains larger than 30% for both the tangential and sagittal directions in the entire field of view. This telescope's working spatial frequency is 57.1 cycles/mm for the 8.75-µm panchromatic pixel and 38.5 cycles/mm for the 13-µm multispectral pixel size. Figure 5 shows a ZEMAX simulation of the ideal MTF for the telescope, with a ray-trace already shown in Figure 1. The MTF is shown for a range of angles relative to the symmetry axis of the system, from 0 to 0.996 deg. As shown in Figure 5, the modulus remains well above 30% throughout the field of view.

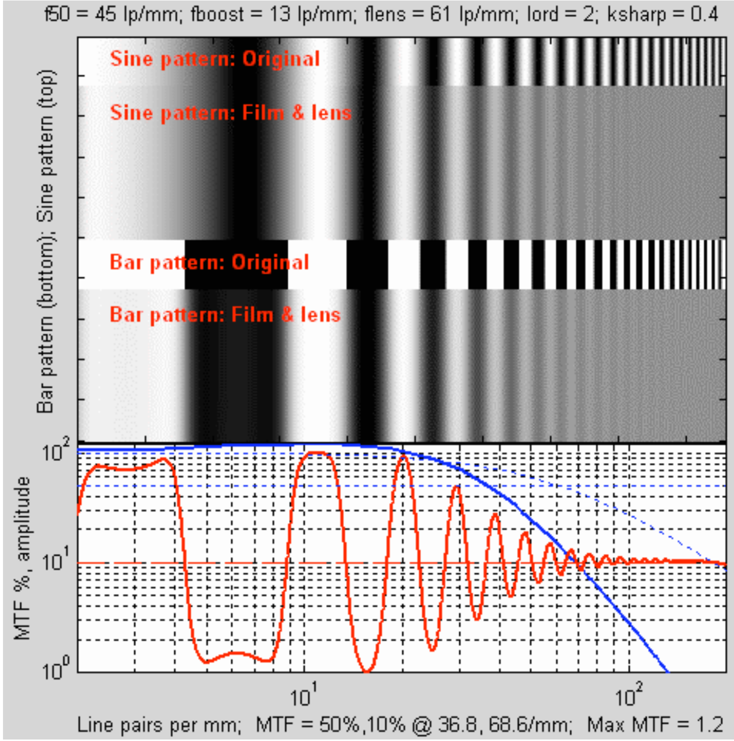

Figure 4. Example of an optical system's capability to image a target. The red curve represents the optic's spatial response to the contrast of the target and the blue line represents the corresponding MTF, where the x-axis measures line pair cycles per millimeter and the y-axis measures the amplitude of modulation as a percentage.

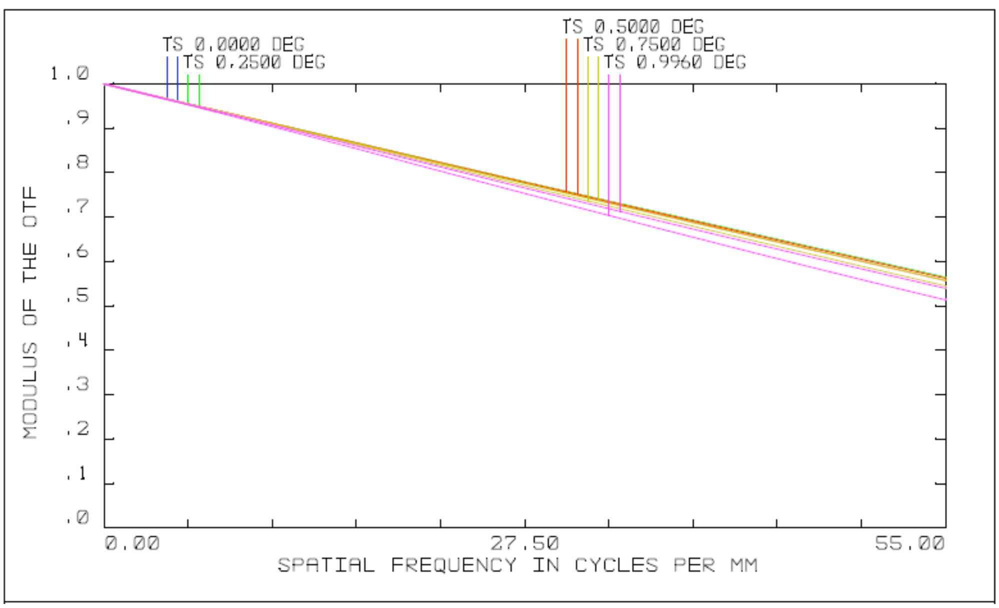

Figure 5. The ideal Modulation Transfer Function for the GoBlue telescope. The tangential and sagittal contrast directions are represented by T and S, respectively. The MTF amplitude is well above the 30% barrier for both panchromatic and multispectral working spatial frequencies for both contrasts directions. The additional MTF amplitude provides the necessary margin required to perform a tolerance analysis of the system.

Figure 6 shows the limitations of the design. The on-axis light converges ideally into the Airy Disk; however, off-axis light near the edge of the FOV is not quite diffraction limited.

3.1 Tolerancing Analysis

A tolerancing analysis has been performed for this system using the tolerancing program within ZEMAX. The objective of this analysis is to provide realistic tolerances for every degree of freedom for each optical surface in the system. The baseline assumption to perform this analysis is that the MTF contrast amplitude may not fall below 30%. The degrees of freedom within the tolerancing program of ZEMAX that affect this system are radius of curvature, thickness (spacing in the z-axis), de-center (x and y-axes, and tilt (x and y-axes). The initial tolerancing conditions used are based on common manufacturing requirements for the given degrees of freedom. These initial tolerances are shown in Table 3.

Table 3. Initial tolerances used to begin tolerancing analysis.

Degree of Freedom	Initial Tolerance
Radius of curvature	±3 fringes
Thickness	±0.2 mm
De-center	±0.1 mm
Tilt	±0.02°

Due to the use of multiple pixel sizes and fields of view used, separate analyses must be completed for panchromatic and multispectral imaging. Monte Carlo simulation runs in the ZEMAX tolerancing program lead to the reduction of these initial tolerances in order to maintain the minimum required MTF contrast amplitude of 30%. Tighter tolerancing is required for this system on the multispectral analysis, as the furthest radial point of the third multispectral CCD sensor extends 4 mm further from the center of the focal plane than does the panchromatic sensor. The extra flat field required to achieve this larger focal plane results in more stringent tolerancing requirements. The tolerances which changed from the initial tolerances in Table 3 are stated in Table 4.

Table 4. Tolerances determined with ZEMAX tolerancing program.

Degree of Freedom	Surface	Surface	Tolerance
Thickness	Primary Mirror	Secondary Mirror	±0.1 mm
	Lens 3, #2	Lens 4, #2	±0.1 mm
	Lens 3, #1	Lens 3, #2	±0.1 mm
	Lens 2, #2	Lens 3, #2	±0.1 mm
De-center	Lens 3, #2	—	±0.05 mm
	Lens 4, #1	—	±0.05 mm
Tilt	Lens 1, #1	—	±0.01°
	Lens 1, #2	—	±0.01°
	Lens 3, #2	—	±0.01°
	Lens 4, #1	—	±0.01°

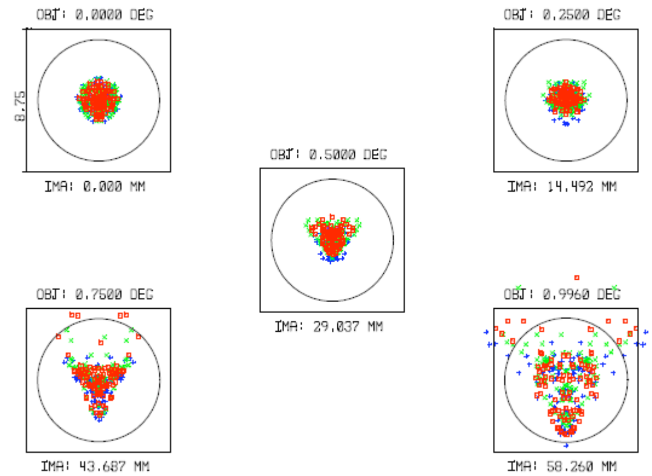

Figure 6. Spot diagram of photons at different locations in the focal plane, denoted as the IMA, or image surface, and measured in millimeters off-axis. Light entering the telescope is denoted by OBJ, or the object surface, and is measured in degrees off-axis. Different colors indicate different frequencies (red=650 nm, green=550 nm, blue=480 nm). All spot diagrams are shown together with the diameter of the Airy disk of the system, representing the diffraction limit, and also in a box equal to the size of the panchromatic pixel.

MTF plots for panchromatic and multispectral imaging with the system performance after applying the tolerances are shown in Figure 7 and 8.

4. Mechanical Considerations

The structural and thermal properties of the spacecraft and telescope are important for the optical performance of the GoBlue telescope. Due to the refractive group used to flatten the field of view, requirements with respect to the suppression of ionizing radiation also have to be considered.

4.1 Structural Design

The mechanical and structural configuration is the result of a lengthy process of optimization coupling static load (i.e., static accelerations), dynamic analysis (modal, shocks, random vibrations, and acoustic) at a structure scale, and optics aspects at a micrometric scale in order to guarantee that the optical components will remain in their positions despite the environment of vibrations and thermal cycles (see Table 1 for thermal range and expected static and vibrational loads). Furthermore, there are important requirements that are highly launch vehicle specific. Here, we designed for the Dnepr launch vehicle, with a longitudinal load of (7.8 ±0.5) g, and a lateral load of (0.5 ±0.5) g. Worst cases were considered here. Furthermore, frequency-dependent vibro-acceleration loads and shock spectra were also considered. For details of these spectra, refer to [12, 13].

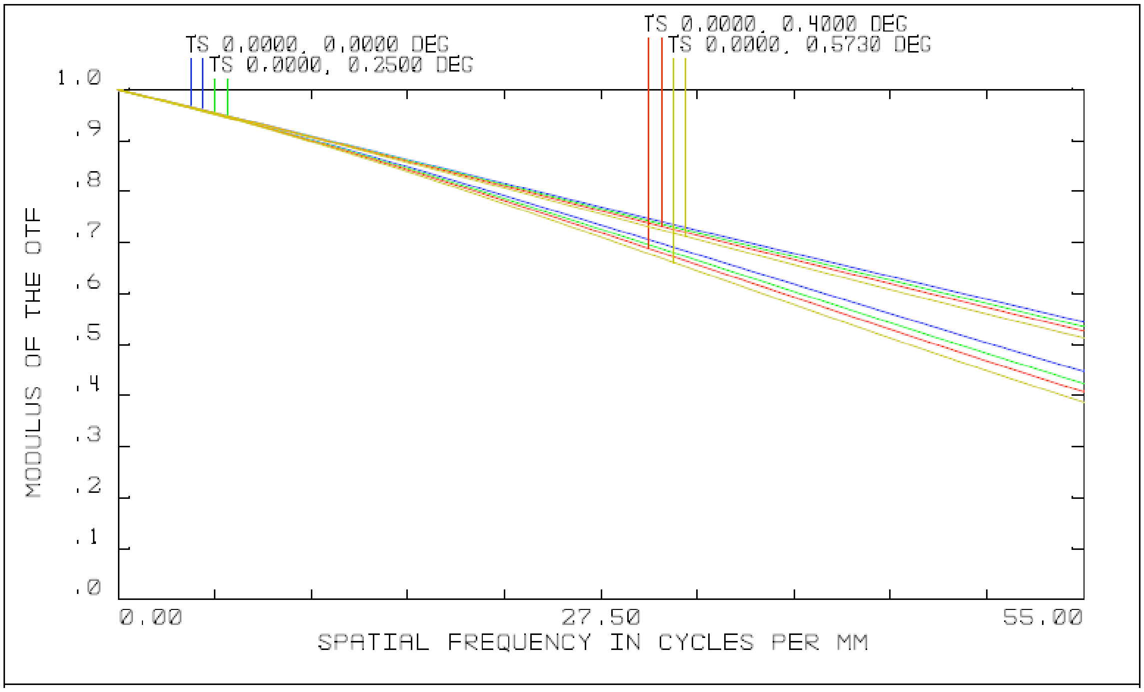

Figure 7. MTF plot showing worst-case contrast amplitudes of panchromatic imaging assuming above stated tolerances are met with no margin.

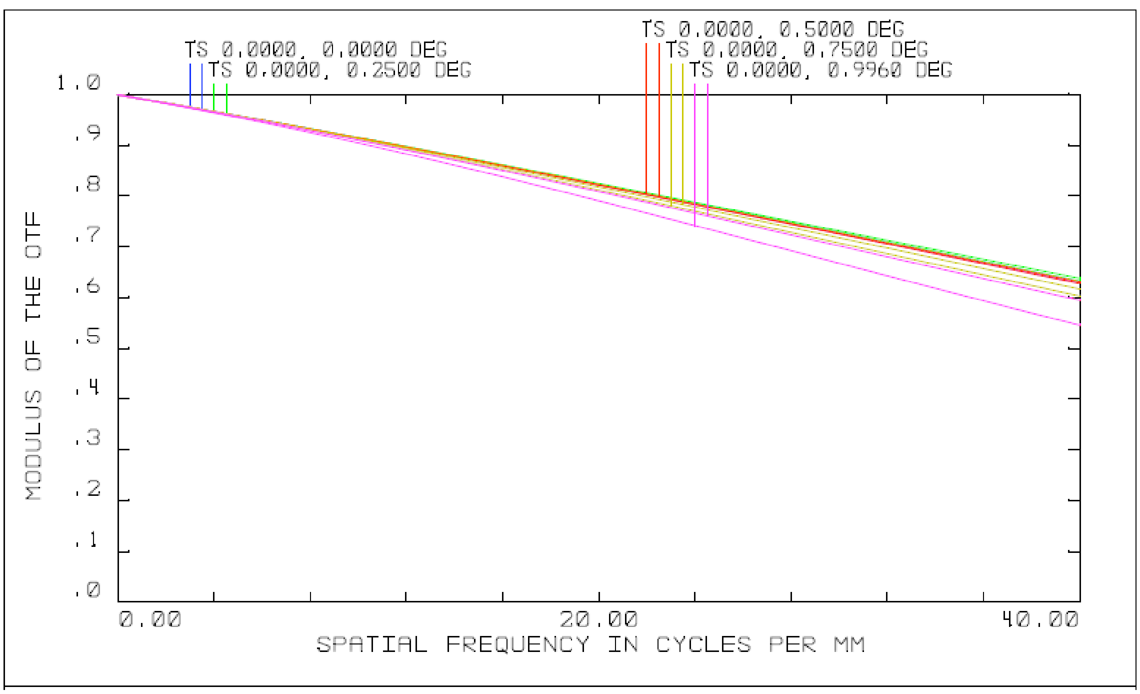

Figure 8. MTF plot showing worst-case contrast amplitude of multispectral imaging assuming above stated tolerances are met with no margin. This plot, although showing no curve near the 30% barrier, had similar Monte Carlo simulations with tolerances slightly relaxed from Table 4 which dip below the barrier.

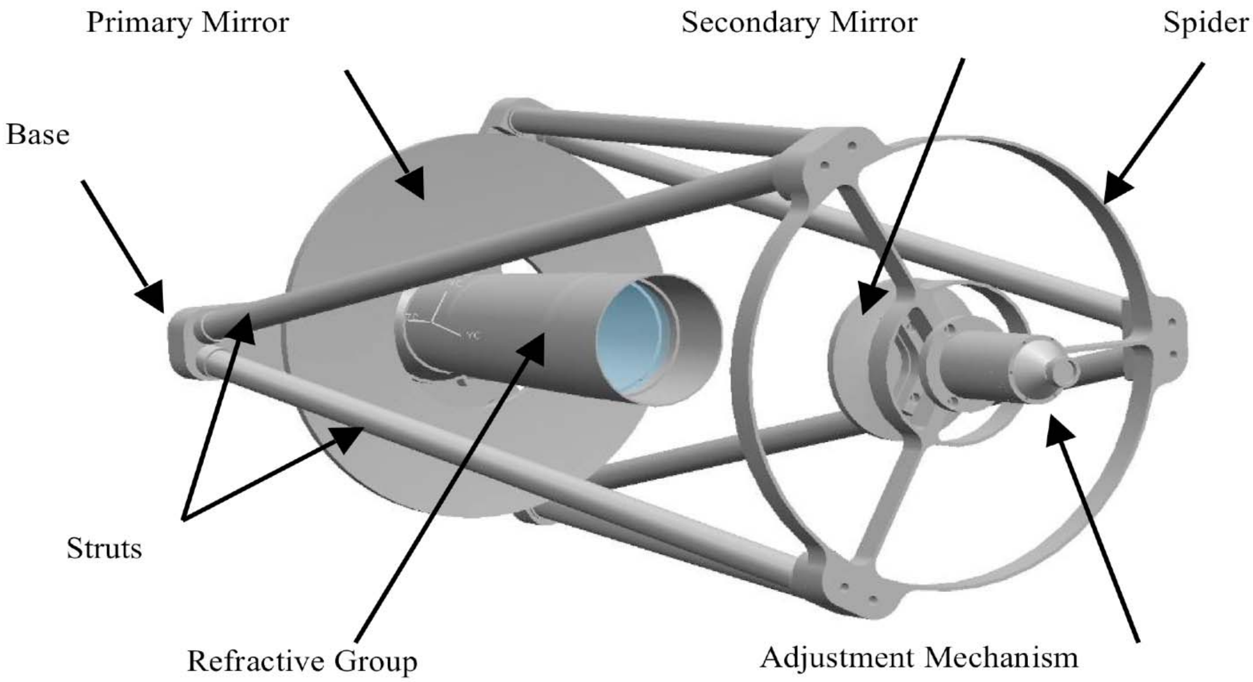

Figure 9. Mechanical design of the GoBlue telescope. For details, refer to text.

Figure 9 shows the baseline design used for the GoBlue telescope. It consists of the base which is the most integral part of the structure. It not only serves as an attachment point from the telescope to the bus, but also supports the primary mirror attachments, the struts that support the spider, the refractive group housing, and the focal plane adjustment mechanism.

A detailed design study was performed to optimize the structural elements (pipes) in Figure 9. Both the number of pipes and their dimension were varied and analyzed in detail. Furthermore, a baseline design was prototyped and run through a thermal and structural test cycle to test the simulation results. A study of several configurations, varying the number of pipes and/or the number of rings, has been performed with the following results. Obviously, the stiffness of the structure is driven by the diameter of the pipes. By increasing the thickness of the pipes the stiffness of the structure decreases because the induced increase of mass increases the inertia to a larger amount than it stiffens it. We also conclude that a three-element geometry (using six pipes) performs better than a four-element geometry (using eight pipes) in terms of the ratio of modal frequency/mass.

Based on these results, a three-fold structure has been chosen. The four-fold structure is more commonly encountered because of gravity issues on the Earth; this configuration allows the mirrors to remain parallel even as the structure deforms, resulting in minimum distortion. In the case of a space-imaging telescope, no gravity aspects will have to be considered once in orbit so it was clear that the three-fold configuration was best.

4.2 Design of Telescope: Static and Dynamic Analysis

The base is at the core of the three-fold symmetry concept. The base links the telescope to the bus, but it also links the maintaining structure of the secondary mirror, the primary mirror, the baffle of the primary mirror, and finally the camera. The base was designed according to the principle of load path minimization—supporting the structure via its attachment to the spacecraft bus as close as possible to the locale of the maximum load. Such an approach minimizes the thickness of the material needed to support the load, and has led to a design with three bus attachment points close to the most massive component of the telescope—the primary mirror. The static stress analysis showed the base having generous margins of safety (3.6 for yield strength, 2.9 for ultimate strength) under 9 g of longitudinal acceleration (the simulation in the radial direction under 2 g revealed an even higher factor of safety). The modal analysis showed that the first two Eigen frequencies were under 100 Hz (27.6 Hz and 66.3 Hz, respectively) mainly driven by the stiffness of the spider but nonetheless sufficiently high to match the criteria of the selected ELV (see specifications of [12, 13]). The harmonic analyses carried out, both in longitudinal and radial directions, in the 2-20 Hz range, have revealed a factor of safety of 3 for the entire structure. The test of random vibrations has revealed that these vibrations were insignificant for the structure (safety factor of 15). Ultimately, the shock simulations turn out to be the most limiting phenomena, essentially for the spider. Several iterations have been carried out for the design of this latter to rigidify it while minimizing the penalty on mass leading to lower Eigen frequencies. The current design has a factor of safety of 3 for the shock profiles of the selected rockets.

4.3. Design of the Primary Mirror and its Support System

The primary mirror is made of Zerodur® glass, which is a material especially used for optical components requiring a low thermal expansion coefficient (between 0.01 and $0.02 \times 10^{-6} K^{-1}$ for Zerodur®) [14]. A great deal of research has been done in the last decade in order to minimize the mass of the primary mirror [15, 16]. These recent technologies have not been considered for this telescope because of their high cost and the complexity introduced to the manufacture of the mirror. Furthermore, the system mass is not one of the key drivers for the GoBlue Imager [1] and reduction of mass, therefore, does not lead to reduction of cost.

The design that has finally been adopted is a so-called "double arch" design. The different studies which have been carried out concerning the optimization of the geometry have revealed that an r/R = 0.7 (ratio of the diameter of the foot of the arch to the diameter of the mirror) yields the best results in terms of weight and surface distortion. The design of the support system of the primary mirror must combine stiffness in the longitudinal direction of the telescope (i.e., in the length direction), but at the same time, needs to be flexible enough in the radial direction. During launch, the accelerations and vibrations are mainly in the longitudinal direction; the supports of the primary mirror were dimensioned so that their yield strength is not reached. Conversely, the supports need to bend easily in the radial direction so that, in case of thermal expansion of the base, the displacement of the supports does not over-constrain the mirror and therefore modify the mirror's curvature.

In order to be perfectly positioned, the mirror has to be maintained by three points, but, given the mass (~16 kg) and the dimensions of the primary mirror it has been determined that six points were better than three points in terms of stiffness and close to the performance of a ring support system. Half spheres are glued at the bottom of the arch. A hole in the middle will allow linking the mirror to its support system. The support system is composed of three identical T-shape sheets of metal of 0.032 aspect ratio. This shape is found to be extremely stiff in the longitudinal direction for compression (direction of the maximum static acceleration) without buckling and supple in the radial direction where it will bend (due to the high aspect ratio). Despite this relative weakness in the radial direction, the symmetrical angular distribution of the support yield ultimately led to a stiff support in the radial direction.

4.4. Design of the Primary Mirror Baffle

The telescope requires the use of four lenses located inside the baffle of the primary mirror, as discussed above. For simplicity and in order to save mass it was decided that the baffle of the primary mirror will house the lenses and their compression support system, as shown in Figure 10. The distance between the lenses will be maintained by carbon fiber spacers whose material properties were chosen considering the relative displacements, modification of the curvature's radius, and coefficient of refraction of the lenses due to thermal variations.

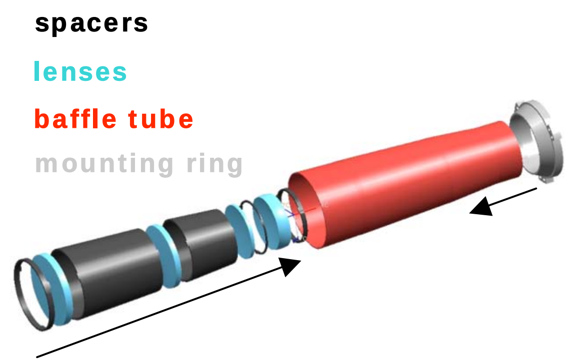

Figure 10. Exploded view of lens compression scheme and primary baffle tubing.

4.5. Design of the Spider and Secondary Mirror

The spider is located at the top of the telescope, which supports the secondary mirror and its positioning mechanism. More specifically, the spider refers to the thin parts (usually sheets of metal) which link the secondary mirror casing to the outer ring, to which the struts are attached.

The design of the spiders is driven by two contradicting requirements: First, spiders have to be as thin as possible to minimize the obstruction. Their number has to be as small as possible because of the diffraction pattern generated in the focal plane. However, the spiders have to be stiff enough so that they will undergo the launch environment (vibrations and accelerations) without reaching the plastic zone of the material so that no collimation will be required during space operation. The geometry of the spiders is designed to match the geometry of the structural elements of the telescope. This minimizes obstructions and simplifies the loading path of the telescope.

The design of the secondary mirror and its adjustment mechanism are important drivers for the optical performance due to the sensitivity of the telescope resolution to the position of the secondary mirror. The position not only has to be guaranteed under vibrations but the length of the support system in the longitudinal direction of the telescope has to be precisely determined so that it will compensate for the overall expansion of the structure in case of variation of the temperature inside the bus. The secondary mirror is made of Zerodur® glass; its shape is a drilled single arch, the hole being used to attach it to the adjustment mechanism (Figure 11).

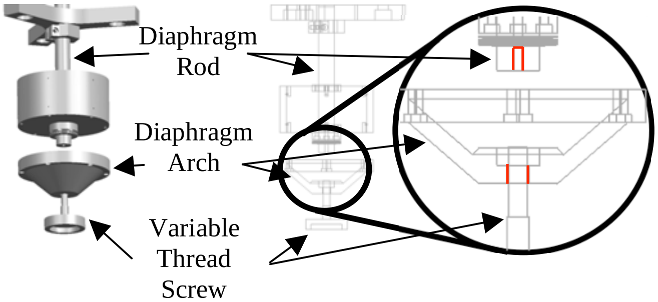

Figure 11. Secondary mirror adjustment mechanism. The symmetric drum-like structure of this mechanism allows the diaphragm rod to be adjusted axially and prevents the possibility of tilting. Axial adjustment as fine as 10 µm is achieved using a differential thread screw (5/16”-24 to ¼”-28).

4.6. Thermal Considerations

In order to minimize the influence of the variation in temperature on the distance between the optical devices, the size of the parts and the type of material has to be optimized so as to make an athermal system. The analysis which is presented here is based on the optimization of the strut length and mechanism of the secondary mirror support so that the distance between the secondary and primary mirrors is unchanged.

As shown in Figure 12, assuming the following thermal expansion coefficients:

1. α_{l1}: The coefficients of thermal expansion (CTE) of the link between the base and the strut,

2. α_{L2}: The link between the strut and the spider,

3. α_L: The CTE of the strut,

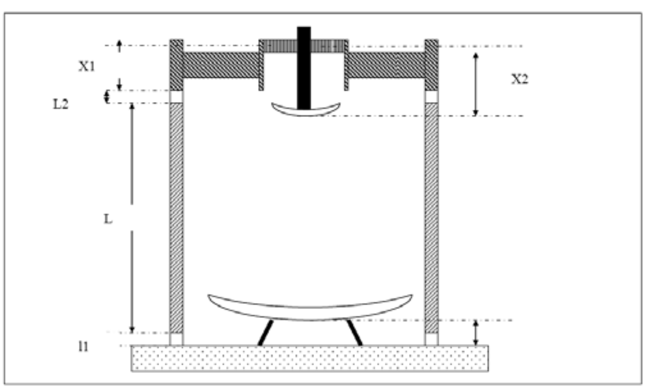

Figure 12. Structural variables considered for the system optimization. For details refer to text.

4. α_s: The CTE of the spider (the ring, the spider itself, and the casing of the secondary mirror system are assumed to be made of the same material),

5. α_r: The CTE of the rod that maintains the secondary mirror by its center,

6. α_P: The CTE of the support of the primary mirror.

The length of all these components are denoted as l_{l1}, l_{l2}, l_L, l_s, l_r, and l_P, respectively. We also assume that ζ is the distance between the secondary and the primary mirror. The objective function is to find the length and material properties of all six components (while respecting manufacturing capabilities and availability of materials) so that $\forall T, \frac{\partial \zeta}{\partial T} = 0$. Hence,

$$\alpha_{l1}l_{l1} + \alpha_L l_L + \alpha_{l2}l_{l2} - \alpha_s l_s - \alpha_r l_r - \alpha_P l_P = 0 .$$

The optimization has to be performed for different types of materials (Ti, Al, carbon, and Invar) and by varying their combinations, the optimization revealed that an athermal structure could be designed using Invar struts and aluminum for the base, the spider, and the support systems of the primary and secondary mirrors.

After preliminary thermal and tolerancing analysis of our telescope, it was determined that two adjustment mechanisms are necessary for a robust optical design. Risk is substantially reduced by incorporating adjustment into our optical design as it allows for alignment correction of sensitive optical components, ensuring pristine performance of the imaging system.

The secondary mirror adjustment mechanism will allow secondary mirror adjustment in the z-axis and also x-y plane tilt capabilities. The mirror mount has three feet on it and, to allow for tilt, these feet can be lapped off to a specified dimension. The spacers can be lapped to an accuracy of 5-10 µm. Since the minimum tolerance for tilt is 0.01 degrees, the adjustment is slightly finer than required by the tolerance. Further detail of the tilt adjustment spacers can be seen in Figure 11. The z-axis adjustment utilizes the remaining parts of this system. The symmetric drum-like structure of this mechanism allows the diaphragm rod to be adjusted axially and prevents the possibility of tilting. This adjustment is made with a 5/16”-24 to ¼”-28 differential thread adjustment screw, which connects the diaphragm arch to the end of the diaphragm rod, as shown in Figure 11. This mechanism allows for adjustments as small as 10 µm in the z direction and a travel of 1.8 mm. The tolerance for this distance is approximately 100 µm, so the adjustment is more than double the accuracy needed to maintain tolerance.

4.7. Ionizing Radiation

Due to the use of the refractive group, care has to be taken to shield from ionizing radiation where possible. The necessary shielding needs to be performed by the mechanical system. The radiation dose received by the GoBlue telescope will be dominated by trapped electrons and protons, as well as high-energy heliospheric radiation. The total dose can be estimated using the European Space Agency Space Environment Information System (SPENVIS) models [17] for a Sun-synchronous orbit at 460-km altitude, and a lifetime of two years.

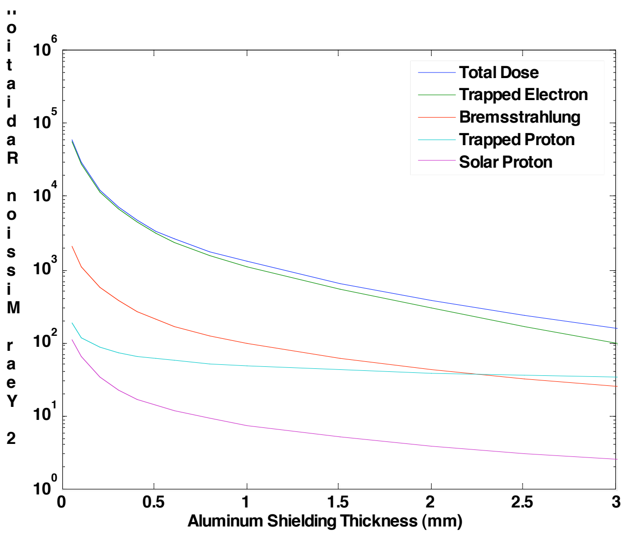

Figure 13. Radiation prediction for radiation components using SPENVIS.

A total shielding of 2 mm Al reduces the radiation to ~200 rads. A detailed analysis of the refractive group suggests that a shielding mass of 3 mm is achieved from all directions, reducing the radiation dose experienced by the first lens below 200 rads. All other lenses have radiation doses during their lifetime below 100 rads. The glasses selected for this design are specified to be resistant to this dose [18].

5. MANUFACTURING AND TEST

The objective of this optical prototype is to prove that a complex optics system can be manufactured at low cost and minimal risk and to determine how well its performance compares to the theoretical model. Several actions have been taken to ensure performance is comparable to what is expected.

An error budget has been kept for every piece of the system. Precise tolerancing of every part and testing procedure is vital to this process and to keep the system on cost. The tolerancing was done to ensure the minimum MTF contrast amplitude remains above 30%. This results in an allowable tolerance for each part of the system.

Based on the large cost to buy custom mirrors and have lens prefabricated, the decision was made to manufacture all optics in house, taking advantage of student labor and campus facilities and machinery, resulting in lens and mirror fabrication costs well below prices quoted from industry. The work involves rough grinding or shaping, as well as polishing. For the mirrors, an additional figuring stage is also required. Figure 14 shows two students grinding lens glass.

Figure 14. Students machining elements of the refractive group.

In addition to the manufacturing processes, testing procedures have also been developed. These procedures include regular measurements with a spherometer and a Heidenhain digital depth gauge [4]. Also, specific three-ball mounts were designed to measure the wedge of lenses. Furthermore, Foucault tests and interferometric tests are used during the polishing stages.

There are specific tests used to gauge the performance of optical elements. The primary mirror is tested with a refractive Offner test, as described in Figure 15. A HeNe laser is used to test the secondary and the integrated system.

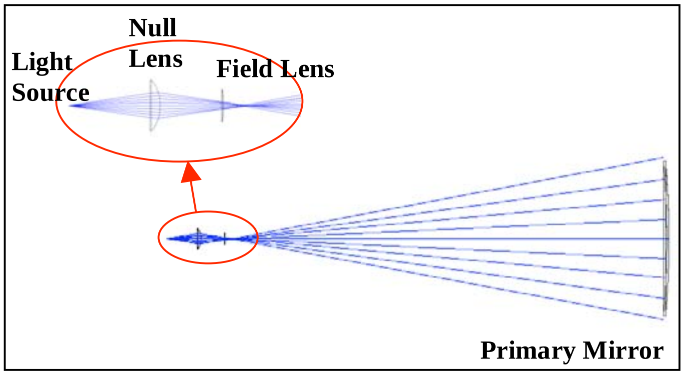

Figure 15. Offner test simulated with ZEMAX.

6. Summary

The GoBlue telescope has been developed for an Earth imaging application designed to image the entire Earth. The primary goal of this prototyping effort was to design this system for minimum cost and to minimize impact on other satellite subsystems. By departing from traditional space imaging applications, the GoBlue team was able to design a highly functional, low-cost telescope that met the mission requirements.

This low-cost design was enabled using a strong reliance on models and prototyping of components. Innovative approaches for adjustment mechanisms have led to substantial reductions in cost leading to a total telescope cost (with only half the CCDs) of $140k.

Furthermore, the telescope construction offered hands-on opportunities for over 20 students at the undergraduate and graduate levels. Students involved in this project have taken the conceptual goals through system requirements, design studies, optimizations, and finally payload prototyping. This effort would not have been possible without their hard work and dedication.

References

[1] T. H. Zurbuchen and R.A. Falor, "Low-Cost Earth Imaging System for Novel Commercial Applications," IEEE Proceedings, this issue, 2007.

[2] A. M. Mika, "Three Decades of Landsat Instruments," PE&RS, 63, 359, 1997.

[3] T. Toutin, "Geometric Processing of Remote Sensing Images: Models, Algorithms, and Methods," Intl. J. Remote Sensing 25, 1893, 2004.

[4] W. J. Smith, Modern Optical Engineering, Third Edition, New York: McGraw-Hill, 2000.

[5] B. Chelsey, R. Lutz, and R.F. Brodsky, "Space Payload Design and Sizing," in Space Mission Analysis and Design, eds. J.R. Wertz and W.J. Larson, New York: Kluwer Academic Press, 1999.

[6]J. R. Wertz and W. J. Larson, Space Mission Analysis and Design, New York: Kluwer Academic Press, 1999.

[7] L. G. Cook, "Three-Mirror Anastigmat used Off-axis in Aperture and Field," in Space Optics, Proc. Soc. Photo-Opt. Instrum. Eng. 183, 207–211, 1979.

[8] C. G. Wynne, "Ritchey-Chretien Telescopes and Extended Field Systems, Astrophys. J. 152, 675, 1968.

[9] R. Reulke, U. Tempelmann, D. Stallmann, M. Cramer, N. Haala, "Improvement of Spatial Resolution with Staggered Arrays as Used in the Airborne Optical Sensor ADS40."

[10] R. Nagura, "SN Improvement Ratio by Time Delay and Integration for High-Resolution Earth Observation Systems," Electronics and Communication in Japan, Part 1, 78, 3, 1995.

[11] http://www.us.schott.com/optics_devices/english/products/flash/abbediagramm_flash.html.

[12] DNEPR, User's Guide, http://snebulos.mit.edu/projects/crm/DNEPR/Dnepr_User_Guide.pdf.

[13] Falcon I, User's Guide: http://www.spacex.com/index.html?section=falcon&content=http%3A//www.spacex.com/falcon_overview.php.

[14] http://www.us.schott.com/optics_devices/english/products/zerodur/index.html.

[15] J. H. Burge, J. R. P. Angel, B. Cuerden, and N. J Woolf, "Glass Membrane Mirrors beyond NGST," in Proceedings, Ultra Lightweight Space Optics Challenge Workshop, http://origins.jpl.nasa.gov/meetings/ulsoc/, Napa, CA, March 24-25, 1999.

[16] http://www.us.schott.com/optics_devices/english/download/tie-38_zerodur_lightweighting_us.pdf.

[17] D. Heynderickx, M. Kruglanski, V. Pierrard, J. Lemaire, M. D. Looper, and J. B. Blake, "A Low-Altitude Trapped Proton Model for Solar Minimum Conditions Based on SAMPEX/PET Data," IEEE Trans. Nucl. Sci. 46, 1475–1480, 1999.

[18] D. B. Doyle and R.H. Czichy, "Influences of Simulated Space Radiation on Optical Glasses," SPIE 2210, 34-448, 1994.

BIOGRAPHY

Thomas H. Zurbuchen *is an Associate Professor of Space Science and Aerospace Engineering at the University of Michigan. He specializes in the heliospheric space environment, and develops and constructs space instruments which are part of numerous spacecraft. Most recently, his group has developed the Fast Imaging Plasma Spectrometer for the Mercury-MESSENGER mission. THZ is also the program advisor for a Masters of Space Engineering program with strong connections to Aerospace Industry. Related to this, he has led space system design efforts with NASA and private industry. He is a recent winner of the Presidential Early Career Award for Scientists and Engineers. He is also the president of Z-Transform, a small University spin-off company providing consulting services.*

Ryan A. Falor *is a graduate student in the Master's in Space Engineering program at the University of Michigan. He is pursuing a career in systems engineering and technical project management. He formerly was a part of the Phoenix payload design team and worked on various studies for the MER, DAWN, and MSL missions while at NASA JPL.*

Romain Clement *is a graduate student in the Master's in Aerospace Engineering program in the Department of Aerospace Engineering at the University of Michigan. He also received a Master's degree in Mechanical Engineering from Ecole Centrale de Lyon, France. He is pursuing a career in systems engineering. Formerly, he was involved in international projects dealing with stability and health monitoring of jet engines.*

Daniel Paul *is a graduate student in the Master's in Space Engineering program at the University of Michigan. He is pursuing a career in space systems with emphasis on optical systems.*

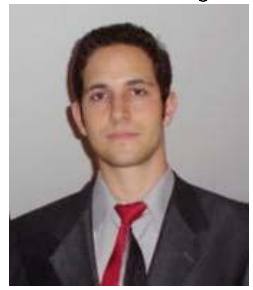

Robby A. Swoish *is a graduate student in the Master's in Space Engineering program at the University of Michigan. He is pursuing a career in space systems engineering.*

Thomas Ryan *is an optical consultant who has designed optical systems for space applications, the military, industry, and the medical field. He is an alumni of the University of Michigan with degrees in Physics and Astronomy, and enjoys spending time with his trophy wife of 23 years, Helen, and bright, hard working students at the University of Michigan.*